Bounds on the effective tensor and the structural parameters for anisotropic two-phase composite material

Engström, Christian

2005

CODEN:LUTEDX/(TEAT-7130)/1-16/(2005)

Bounds on the effective tensor and the structural parameters for anisotropic two-phase composite material

Christian Engström

Department of Electroscience
Electromagnetic Theory
Lund Institute of Technology
Sweden

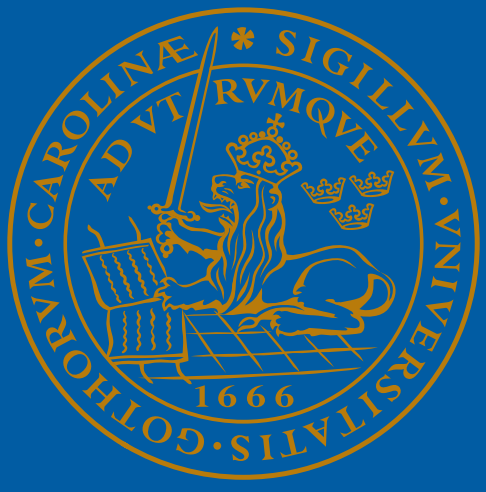

Christian Engström

Department of Electroscience
Electromagnetic Theory
Lund Institute of Technology
P.O. Box 118
SE-221 00 Lund
Sweden

Editor: Gerhard Kristensson

Abstract

A new method to estimate the microstructural parameters of anisotropic two-phase composite material is derived. The parameters are estimated using information from measurements or from numerical experiments. The method is used to derive new bounds on the effective tensor that incorporates information from measurements of a related parameter. These new bounds are called cross-property bounds. New tight bounds on low-order microstructural parameters are given in the anisotropic case.

1 Introduction

The problem of determining the effective properties of a composite is classical in physics and engineering. The determination of the effective permittivity tensor is the focus of this article, but the results work equally well for the effective thermal conductivity, magnetic permeability or diffusivity of the composite material. In many instances the inhomogeneities in the composite material are small compared with the wavelength. The composite then reacts to the slowly varying field in much the same way as a homogeneous material. In this case an effective permittivity tensor $\boldsymbol{\epsilon}^{\text{eff}}$ is given by

$$\langle \boldsymbol{D} \rangle = \langle \boldsymbol{\epsilon} \boldsymbol{E} \rangle = \boldsymbol{\epsilon}^{\text{eff}} \langle \boldsymbol{E} \rangle, \tag{1.1}$$

which relates the average, $\langle \cdot \rangle$, of the electric displacement field $\langle \boldsymbol{D} \rangle$ to the average of the electric field $\langle \boldsymbol{E} \rangle$. The material is usually assumed to be statistically homogeneous. Roughly speaking, the material is statistically homogeneous if different parts of the sample have the same statistical properties [4]. The volume averages can then be replaced by ensemble averages.

The effective permittivity can be determined by solving a local problem in the form of a partial differential equation [2, p. 663]. Fast and accurate numerical methods to solve this differential equation have been developed in recent years [13, 14]. In two dimensions it is possible to calculate problems with thousands of inclusions, which give accurate estimates on the effective permittivity in the stochastic case [14]. One drawback is that a complete knowledge of the geometry rarely is available. Another drawback with this approach is that the problem depends not only on the microstructure but also on the contrast. If we change the contrast all calculations need to be repeated.

An alternative approach is to characterize the microstructure in terms of an infinite set of correlation functions [4, 9]. Except for some special cases the infinite set of correlation functions are not known and hence an exact solution is not possible. If some of the correlation functions are known this knowledge can be used to obtain rigorous bounds on the effective property. The bounds become progressively narrower as more microstructural information is used.

In the case of macroscopically isotropic materials, considerable theoretical progress has been made, see for example [4–6, 11, 18–20, 22] and the monographs [21, 29]. The case of macroscopically anisotropic materials are less studied. Theoretical works

include [16, 19, 20, 25, 27], see also the monographs [21, 29]. The microstructural parameters in the anisotropic case are harder to determine and have only been calculated in a few special cases [24, 28].

In this article we provide new tight bounds on the microstructural parameters and bounds on the effective permittivity for loosy materials (complex-valued permittivity). Moreover, we provide a new method to estimate the microstructural parameters using measurements or the solution of the local problem [2, p. 663]. The local problem is solved for a low contrast, but the bounds are valid for all contrasts. One of the bounds can in many cases provide an accurate estimate of the effective permittivity even when the lower and upper bounds are very distant from each other. Finally, we give new bounds in the anisotropic case that incorporates information from measurements, so called cross-property bounds.

This paper is organized as follows. Section 2 presents notation and bounds used in this paper. A method for determination of the structural parameters is given in Section 3. In Section 4 bounds on the structural parameters are derived. Section 5 gives complex bounds on the permittivity in the anisotropic case. Cross-property bounds are calculated in Section 6. Finally, the results are discussed in Section 7.

2 Preliminaries

The materials in this paper are assumed to be d-dimensional and to consist of two homogenous, isotropic phases. The two-component material is locally modeled by the scalar relative permittivity

$$\epsilon(\epsilon_1, \epsilon_2) = \epsilon_1 \chi_1(\boldsymbol{x}) + \epsilon_2 \chi_2(\boldsymbol{x}), \tag{2.1}$$

where the components are isotropic with constant permittivity ϵ_1 and ϵ_2. The volume fraction of the two phases are denoted f_1, f_2, respectively and the characteristic function χ_i is defined as

$$\chi_i(\boldsymbol{x}) = \begin{cases} 1, & \boldsymbol{x} \text{ in phase } i \\ 0, & \text{otherwise.} \end{cases}$$

The effective permittivity matrix is written as the power series expansion

$$\frac{\boldsymbol{\epsilon}^{\text{eff}}}{\epsilon_2} = \mathbf{F}(z), \qquad \mathbf{F}(z) = \sum_{n=0}^{\infty} \mathbf{c}_n z^n \tag{2.2}$$

where $z = (\epsilon_1 - \epsilon_2)/\epsilon_2$ is the contrast. The matrices $\mathbf{c}_n$ can be calculated from integrals over the correlation functions $S_1, \ldots, S_n$ associated with the phase 1. The n-point correlation function is defined by the ensemble average

$$S_n(\boldsymbol{x}_1, \ldots, \boldsymbol{x}_n) = \langle \chi_1(\boldsymbol{x}_1)\chi_1(\boldsymbol{x}_2) \ldots \chi_1(\boldsymbol{x}_n) \rangle \tag{2.3}$$

that gives the probability of finding n points with positions $\boldsymbol{x}_1, \ldots, \boldsymbol{x}_n$ all in phase 1, see [19–21, 25]. The correlation functions are possible to calculate from photographs of cross sections using image analyses, see [29, Chapter 12].

2.1 Bounds on the eigenvalues of the effective permittivity matrix

Rigorous bounds on the effective permittivity can be obtained for example using variational principles [11, 21], compensated compactness [21, Chapter 24] or explicit representation formulas [6, 19, 20]. The key idea to the last method is that the effective permittivity is a special analytic function that can be written as a Stieltjes function. Stieltjes functions have known upper and lower bounds in the form of continued fractions or Padé approximations. We use Padé approximations of the power series (2.2) when the structural parameters $\mathbf{c}_n$ possess common principal axes. This excludes materials where the principal axis of $\boldsymbol{\epsilon}^{\text{eff}}$ rotate as the contrast changes, see [15].

Let ϵ^{eff} be one of the eigenvalues of the matrix $\boldsymbol{\epsilon}^{\text{eff}} = \epsilon_2 \mathbf{F}(z)$. The $\epsilon_{p,q}$ Padé approximant is defined as

$$\epsilon_{p,q} = \frac{a_0 + ... + a_p z^p}{1 + b_1 z + ... b_q z^q} \tag{2.4}$$

whose Taylor series agrees with that of ϵ^{eff} up to order $p+q$, see [1]. Certain Padé approximations of $\boldsymbol{\epsilon}^{\text{eff}}$ give bounds on $\boldsymbol{\epsilon}^{\text{eff}}$, see [15]. When $\epsilon_2 \geq \epsilon_1$ and $N \geq 1$, the N-point upper bounds $\boldsymbol{\epsilon}_N^{\text{U}}$ are obtained by forming the approximations

$$\boldsymbol{\epsilon}_{2M+1}^{\text{U}} = \epsilon_2 \boldsymbol{\epsilon}_{M+1,M}(\mathbf{F}), \quad \boldsymbol{\epsilon}_{2M}^{\text{U}} = \epsilon_2 \boldsymbol{\epsilon}_{M,M}(\mathbf{F}) \tag{2.5}$$

where the first two coefficients in the Taylor series $\mathbf{F}$ are $\mathbf{c}_0 = \mathbf{I}$ and $\mathbf{c}_1 = f_1 \mathbf{I}$, see [6, 21].

Lower bounds on $\boldsymbol{\epsilon}^{\text{eff}}$ are given from Padé approximations of the series

$$\left(\frac{\boldsymbol{\epsilon}^{\text{eff}}}{\epsilon_1}\right)^{-1} = \tilde{\mathbf{F}}(z), \quad \text{where} \quad \tilde{\mathbf{F}}(z) = \sum_{n=0}^{\infty} \tilde{\mathbf{c}}_n z^n. \tag{2.6}$$

The coefficients $\mathbf{c}_n$ and $\tilde{\mathbf{c}}_n$ are related according to

$$\tilde{\mathbf{c}}_0 = \mathbf{I}, \quad \tilde{\mathbf{c}}_1 = f_2 \mathbf{I}, \quad \tilde{\mathbf{c}}_n = -\sum_{k=0}^{n-1} \tilde{\mathbf{c}}_k \mathbf{c}_{n-k}. \tag{2.7}$$

The N-point lower bounds $\boldsymbol{\epsilon}_N^{\text{L}}$, when $\epsilon_2 \geq \epsilon_1$ and $N \geq 1$, are obtained from

$$\boldsymbol{\epsilon}_{2M+1}^{\text{L}} = \epsilon_1 \boldsymbol{\epsilon}_{M+1,M}^{-1}(\tilde{\mathbf{F}}), \quad \boldsymbol{\epsilon}_{2M}^{\text{L}} = \epsilon_1 \boldsymbol{\epsilon}_{M,M}^{-1}(\tilde{\mathbf{F}}). \tag{2.8}$$

In the following subsections we present the N-point bounds for $N = 1, 2, 3, 4$. The contrast is $z = (\epsilon_1 - \epsilon_2)/\epsilon_2$ and $\epsilon_2 \geq \epsilon_1$ in all cases.

2.1.1 One-point bounds

The $\boldsymbol{\epsilon}_{1,0}$ Padé approximant of the expansion (2.6) gives the lower bound

$$\boldsymbol{\epsilon}_1^{\text{L}} = \frac{\epsilon_1}{1 + f_2 z} \mathbf{I} = \left(\frac{f_1}{\epsilon_1} + \frac{f_2}{\epsilon_2}\right)^{-1} \mathbf{I} \tag{2.9}$$

and the $\boldsymbol{\epsilon}_{1,0}$ Padé approximant of (2.2) gives the upper bound

$$\boldsymbol{\epsilon}_1^{\mathrm{U}} = (\epsilon_2 + f_1\epsilon_2 z)\mathbf{I} = (f_1\epsilon_1 + f_2\epsilon_2)\mathbf{I}. \tag{2.10}$$

These bounds, first derived by Wiener [30], show us that the permittivity is bounded between the harmonic and arithmetic means.

2.1.2 Two-point bounds

The $\boldsymbol{\epsilon}_{1,1}$ Padé approximant of the expansion (2.6) gives the lower bound

$$\boldsymbol{\epsilon}_2^{\mathrm{L}} = \epsilon_1[f_2\mathbf{I} - \tilde{\mathbf{c}}_2 z][f_2\mathbf{I} - \tilde{\mathbf{c}}_2 z + f_2^2 z\mathbf{I}]^{-1} \tag{2.11}$$

where $\tilde{\mathbf{c}}_2 = -\mathbf{c}_2 - f_1 f_2\mathbf{I}$. The $\boldsymbol{\epsilon}_{1,1}$ Padé approximant of (2.2) gives the upper bound

$$\boldsymbol{\epsilon}_2^{\mathrm{U}} = \epsilon_2[f_1\mathbf{I} - \mathbf{c}_2 z + f_1^2 z\mathbf{I}][f_1\mathbf{I} - \mathbf{c}_2 z]^{-1}. \tag{2.12}$$

These bounds were first derived in [16, 27].

In the isotropic case $\mathbf{c}_2 = -(f_1 f_2/d)\mathbf{I}$ the two-point bounds are equivalent to the Hashin-Shtrikman bounds [11].

2.1.3 Three-point bounds

The $\boldsymbol{\epsilon}_{2,1}$ Padé approximation of the expansions (2.6) and (2.2) gives the lower and upper bounds

$$\boldsymbol{\epsilon}_3^{\mathrm{L}} = \epsilon_1[\tilde{\mathbf{c}}_2 - \tilde{\mathbf{c}}_3 z][\tilde{\mathbf{c}}_2 + \tilde{\mathbf{c}}_2 f_2 z + \tilde{\mathbf{c}}_2^2 z^2 - \tilde{\mathbf{c}}_3 z(1 + f_2 z)]^{-1}, \tag{2.13}$$

$$\boldsymbol{\epsilon}_3^{\mathrm{U}} = \epsilon_2[\mathbf{c}_2 + \mathbf{c}_2 f_1 z + \mathbf{c}_2^2 z^2 - \mathbf{c}_3 z(1 + f_1 z)][\mathbf{c}_2 - \mathbf{c}_3 z]^{-1}. \tag{2.14}$$

The coefficients are related according to

$$\tilde{\mathbf{c}}_2 = -\mathbf{c}_2 - f_1 f_2\mathbf{I}, \quad \tilde{\mathbf{c}}_3 = -\mathbf{c}_3 - f_2\mathbf{c}_2 - \tilde{\mathbf{c}}_2 f_1. \tag{2.15}$$

In the case of an isotropic media we have $\mathbf{c}_2 = -(f_1 f_2/d)\mathbf{I}$ and $\mathbf{c}_3 = f_1 f_2 d^{-2}(f_2 + (d-1)\zeta_1)\mathbf{I}$. The anisotropic three-point bounds then reduces to the Beran bounds [3, 26], involving the structural parameters ζ_1 and ζ_2 where $\zeta_1 + \zeta_2 = 1$. In terms of correlation functions, the ζ_1 parameter can, in the three-dimensional case, be calculated from

$$\zeta_1 = \frac{9}{2f_1 f_2}\int_0^\infty \mathrm{d}r \int_0^\infty \mathrm{d}s \int_{-1}^{+1} \mathrm{d}u \frac{S_3(r,s,u)}{rs} P_2(u) \tag{2.16}$$

where $P_2(u)$ is the Legendre polynomial of order 2 and $S_3(r,s,u)$ is the probability of a triangle, with two sides of length r and s with common angle $\cos^{-1}(u)$, having all three vertices lie in the component 1 material when placed randomly in the composite, *i.e.*, varied over all translations and solid-body rotations of the triangle.

2.1.4 Four-point bounds

The $\boldsymbol{\epsilon}_{2,2}$ Padé approximant of the expansion (2.6) gives the lower bound

$$\boldsymbol{\epsilon}_4^{\mathrm{L}} = \epsilon_1 \tilde{\mathbf{P}}_2 \tilde{\mathbf{Q}}_2^{-1} \tag{2.17}$$

where the two polynomials are

$$\tilde{\mathbf{P}}_2 = \tilde{\mathbf{c}}_2^2 - \tilde{\mathbf{c}}_3 f_2 + \tilde{\mathbf{c}}_4 f_2 z + \tilde{\mathbf{c}}_3^2 z^2 - \tilde{\mathbf{c}}_2 z(\tilde{\mathbf{c}}_3 + \tilde{\mathbf{c}}_4 z), \tag{2.18}$$

$$\begin{aligned} \tilde{\mathbf{Q}}_2 = {} & \tilde{\mathbf{c}}_2^3 z^2 + \tilde{\mathbf{c}}_3^2 z^2 + \tilde{\mathbf{c}}_2^2(1 + f_2 z) - \tilde{\mathbf{c}}_3 f_2(1 + f_2 z) \\ & + \tilde{\mathbf{c}}_4 f_2 z(1 + f_2 z) - \tilde{\mathbf{c}}_2 z(\tilde{\mathbf{c}}_3 + \tilde{\mathbf{c}}_4 z + 2\tilde{\mathbf{c}}_3 f_2 z). \end{aligned} \tag{2.19}$$

The coefficients are related according to (2.7). The $\boldsymbol{\epsilon}_{2,2}$ Padé approximant of the expansion (2.2) gives the upper bound

$$\boldsymbol{\epsilon}_4^{\mathrm{U}} = \epsilon_2 \mathbf{P}_2 \mathbf{Q}_2^{-1} \tag{2.20}$$

where

$$\begin{aligned} \mathbf{P}_2 = {} & \mathbf{c}_2^3 z^2 + \mathbf{c}_3^2 z^2 + \mathbf{c}_2^2(1 + f_1 z) - \mathbf{c}_3 f_1(1 + f_1 z) \\ & + \mathbf{c}_4 f_1 z(1 + f_1 z) - \mathbf{c}_2 z(\mathbf{c}_3 + \mathbf{c}_4 z + 2\mathbf{c}_3 f_1 z), \end{aligned} \tag{2.21}$$

$$\mathbf{Q}_2 = \mathbf{c}_2^2 - \mathbf{c}_3 f_1 + \mathbf{c}_4 f_1 z + \mathbf{c}_3^2 z^2 - \mathbf{c}_2 z(\mathbf{c}_3 + \mathbf{c}_4 z). \tag{2.22}$$

In the isotropic case these bounds reduce to the Milton bounds [18]. The Milton bounds depend on the three-point parameter ζ_1 in (2.16) and a four-point parameter, see [29, p. 562].

3 Bounds on the structural parameters using lower order parameters

Let c_n be one of the diagonal elements in $\mathbf{c}_n$. In [25], Sen and Torquato obtained upper and lower bounds on c_2 and a lower bound on c_3. In [29], Torquato derived an upper bound on c_3. We use a powerful method to get a simple proof of the bounds on c_2, c_3 and to derive bounds on c_4. We simply use that when varying the free parameter c_n in the n-point bounds, the bounds are forbidden to violate the $(n-1)$-bounds. We have equality for some value on c_n, that provides a bound on the parameter. In the next sections, we determine if the function $\epsilon_{p,q}(c_n)$ is an increasing or decreasing function of c_n. This determines if the extreme value is a minimum or a maximum. We use this method for all the bounds in the previous section.

The volume fraction c_1 is of course bounded between zero and one. The bounds ϵ_2^{L} and ϵ_1^{U} are equal when $c_2 = 0$ and the bounds ϵ_2^{L} and ϵ_1^{L} are equal when $c_2 = -f_1 f_2$. This gives us the inequality

$$-f_1 f_2 \leq c_2 \leq 0. \tag{3.1}$$

The relation between the coefficients (2.15) implies $-f_1 f_2 \leq \tilde{c}_2 \leq 0$. In [25], the authors give a more complicated proof of this inequality. In the same way, by calculating when $\epsilon_3^{\mathrm{L}} = \epsilon_2^{\mathrm{L}}$ and $\epsilon_3^{\mathrm{L}} = \epsilon_2^{\mathrm{U}}$, we get the inequality

$$c_3^{\min} \leq c_3 \leq c_3^{\max} \tag{3.2}$$

where the end points are

$$c_3^{\min} = \frac{c_2^2}{f_1}, \quad c_3^{\max} = -c_2\left(1 + \frac{c_2}{f_2}\right). \tag{3.3}$$

Relation (2.15) and the extreme values (3.3) give us the inequality

$$-\tilde{c}_2\left(1 + \frac{\tilde{c}_2}{f_1}\right) \leq \tilde{c}_3 \leq \frac{\tilde{c}_2^2}{f_2}. \tag{3.4}$$

That we have obtained the correct end points are easily checked. The bounds ϵ_3^L and ϵ_2^L are equal when $c_3 = c_3^{\max}$ and $\epsilon_3^L = \epsilon_2^U$ when $c_3 = c_3^{\min}$.

Solving $\epsilon_4^{\mathrm{L}} = \epsilon_3^{\mathrm{L}}$ with respect to c_4 give us the lower bound $c_4^{\min}$. The algebraic calculations are harder in the upper bound case. To simplify the algebraic calculations $\epsilon_4^{\mathrm{U}} = \epsilon_3^{\mathrm{U}}$ is solved with respect to $\tilde{c}_4$. Relation (2.7) then gives the upper bound on c_4. The result is given by

$$c_4^{\min} \leq c_4 \leq c_4^{\max} \tag{3.5}$$

where

$$c_4^{\min} = \frac{c_2^3 + f_2 c_2^2 + c_2 c_3(f_2 - f_1) + c_3(c_3 - f_1 f_2)}{c_2 + f_1 f_2}, \quad c_4^{\max} = \frac{c_3^2}{c_2}. \tag{3.6}$$

Relation (2.7) and the extreme values (3.6) give us the inequality

$$\frac{\tilde{c}_3^2}{\tilde{c}_2} \leq \tilde{c}_4 \leq \frac{\tilde{c}_2^3 + f_1 \tilde{c}_2^2 + \tilde{c}_2 \tilde{c}_3(f_1 - f_2) + \tilde{c}_3(\tilde{c}_3 - f_2 f_1)}{\tilde{c}_2 + f_2 f_1}. \tag{3.7}$$

The same procedure can be used to limit higher order structural parameters, c_n.

4 Bounds on the structural parameters using measured or calculated values of ϵ^{eff}

In [17], Lord Rayleigh's technique and a certain differentiation were used to determine bounds for a material composed of disks placed in a square or hexagonal array. In [7], the Fourier transform and a continued-fraction expansion were used to produce numerical bounds on the effective parameters. In [12], the author introduced a numerical method based on the fast multipole method and the conjugate gradient method to solve the equations in [17]. The method is shown to be very effective in the case of nearly touching disks. Numerical calculations of the structural parameters ζ_1 and μ_1 have been done with high accuracy for disks and spheres [12].

The structural parameters for macroscopically anisotropic media are less studied. In one case, where the anisotropy is the consequence of the shape of the inclusions

the structural parameter $\mathbf{c}_2$ was calculated [28]. The authors compute two-point bounds for a distribution of oriented overlapping cylinders, with a finite aspect ratio. Two-point bounds for anisotropic second-rank laminates are found in [24].

Here we propose a method to get numerical bounds on the structural parameters $\mathbf{c}_1$, $\mathbf{c}_2$ and $\mathbf{c}_3$ from computations or measurements. Moreover, this section provide the basis for the cross-property bounds in Section 6. The functions $\epsilon_{p,q}(c_n)$ in this section are defined on the line segment $l = \{c_n; c_n^{\min} \leq c_n \leq c_n^{\max}\}$ from Section 3. The expressions are simplified using Mathematica 5 (`www.wolfram.com`).

4.1 One-point bounds

Write the arithmetic mean (2.10) as $\epsilon_1^{\mathrm{U}}(c_1; \epsilon_1, \epsilon_2) = c_1\epsilon_1 + (1 - c_1)\epsilon_2$. Regard this upper bound ϵ_1^{U} and the lower bound (2.9) as functions of the single variable c_1 alone. Assume that $\epsilon_2 > \epsilon_1 > 0$. The c_1-dependent functions

$$\epsilon_1^{\mathrm{L}} : [0, 1] \to [\epsilon_1, \epsilon_2], \quad \epsilon_1^{\mathrm{U}} : [0, 1] \to [\epsilon_1, \epsilon_2] \tag{4.1}$$

are then bijections and they have decreasing inverses. This gives $(\epsilon_1^{\mathrm{U}})^{-1}(\epsilon^{\mathrm{eff}}) \geq c_1$ and $(\epsilon_1^{\mathrm{L}})^{-1}(\epsilon^{\mathrm{eff}}) \leq c_1$, which are upper and lower bounds on c_1, denoted by $c_1^{\mathrm{U}} := (\epsilon_1^{\mathrm{U}})^{-1}(\epsilon^{\mathrm{eff}}) \geq c_1$ and $c_1^{\mathrm{L}} := (\epsilon_1^{\mathrm{L}})^{-1}(\epsilon^{\mathrm{eff}}) \leq c_1$, respectively. The procedure is illustrated in Figure 1. Explicitly the parameter c_1 is bounded by $c_1^{\mathrm{L}} \leq c_1 \leq c_1^{\mathrm{U}}$ where

$$c_1^{\mathrm{L}} = \frac{1/\epsilon^{\mathrm{eff}} - 1/\epsilon_2}{1/\epsilon_1 - 1/\epsilon_2}, \quad c_1^{\mathrm{U}} = \frac{\epsilon_2 - \epsilon^{\mathrm{eff}}}{\epsilon_2 - \epsilon_1}. \tag{4.2}$$

These bounds on the volume fraction $c_1 = f_1$ can be very narrow in the case of a low or high contrast material. Let $\epsilon_1 = 1$ and $\epsilon_2 = 1 + \delta$. Using the expansion (2.2) the asymptotic behavior when $\delta \to 0$ is

$$c_1^{\mathrm{U}} - c_1^{\mathrm{L}} = f_1 f_2 \delta + O(\delta^2). \tag{4.3}$$

For a fixed δ, the difference is smaller when the volume fraction is low or high, *i.e.*, when the c_1 parameter is close to the end points $c_1^{\min} = 0$ and $c_1^{\max} = 1$.

The one-point bounds can for example be used to check the volume fraction in experiments where it is sometimes difficult to determine the fraction from direct measurements.

4.2 Two-point bounds

Denote by c_2 one of the diagonal elements in $\mathbf{c}_2$. Using $\tilde{c}_2 = -c_2 - f_1 f_2$, the two-point lower and upper bounds then are

$$\epsilon_2^{\mathrm{L}} = \epsilon_1 \frac{(c_2 + f_1 f_2)(\epsilon_2 - \epsilon_1) - f_2\epsilon_2}{c_2(\epsilon_2 - \epsilon_1) - f_2\epsilon_1} \tag{4.4}$$

and

$$\epsilon_2^{\mathrm{U}} = \epsilon_2 \frac{c_2(\epsilon_2 - \epsilon_1) + f_1\langle\epsilon\rangle}{f_1\epsilon_2 + c_2(\epsilon_2 - \epsilon_1)}. \tag{4.5}$$

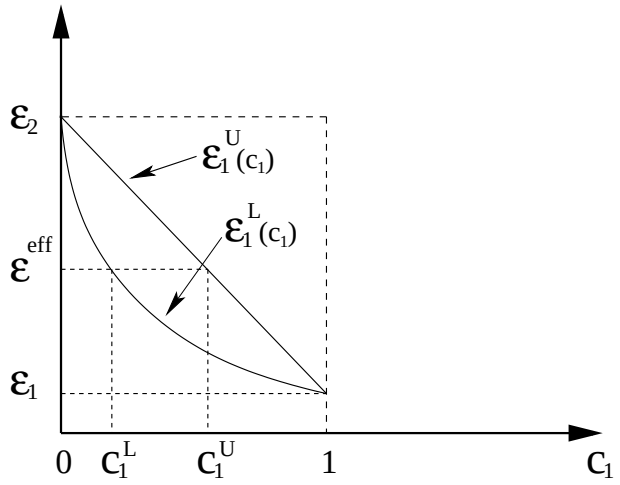

Figure 1: From a known value of ϵ^{eff} and the bounds ϵ_2^{L}, ϵ_2^{U} we get bounds on the structural parameter c_1.

The term $\langle\epsilon\rangle$ denotes here the arithmetic mean $f_1\epsilon_1 + f_2\epsilon_2$.

One way of calculating c_2 is by using the Taylor expansion of the effective permittivity ϵ^{eff} given in (2.2). This gives

$$c_2 = \frac{1}{2}\frac{\partial^2\epsilon^{\text{eff}}(1,1)}{\partial\epsilon_1^2}, \tag{4.6}$$

and shows that c_2 can be computed by varying the phases for weak contrasts. The number of computations needed depends on the formula chosen for numerical differentiation. We need at least three points but if the difference between the permittivities ϵ_1 and ϵ_2 is too small, it is hard to get high accuracy on ϵ^{eff}. To get higher accuracy a higher order scheme can be used, but even then the accuracy is in many cases poor when the c_2 parameter is small. This is a bad method from a numerical point of view. The technique in [12, 17] is much better but here we suggest another approach, providing bounds on c_2 rather than a direct calculation.

Let $\epsilon_2 > \epsilon_1 > 0$ and regard $\epsilon_2^{\text{U}}(c_2; \epsilon_1, \epsilon_2, f_1)$ as a function of c_2 alone. The continuous function

$$\epsilon_2^{\text{U}} : [-f_1 f_2, 0] \to [\epsilon_1^{\text{L}}, \epsilon_1^{\text{U}}] \tag{4.7}$$

is a bijection. It is simple to show that ϵ_2^{U} is one to one and that it is onto follows from $(\epsilon_2^{\text{U}})'(c_2) > 0$, $\epsilon_2^{\text{U}}(-f_1 f_2) = \epsilon_1^{\text{L}}$ and $\epsilon_2^{\text{U}}(0) = \epsilon_1^{\text{U}}$. Since $(\epsilon_2^{\text{U}})^{-1}$ is an increasing function, we have $c_2^{\text{L}} := (\epsilon_2^{\text{U}})^{-1}(\epsilon^{\text{eff}}) \le c_2$. Using ϵ_2^{L} we obtain in the same way an upper bound c_2^{U}. Explicitly, the parameter c_2 is bounded by $c_2^{\text{L}} \le c_2 \le c_2^{\text{U}}$ where

$$c_2^{\text{L}} = \frac{\epsilon_2 f_1(\epsilon^{\text{eff}} - \langle\epsilon\rangle)}{(\epsilon_2 - \epsilon_1)(\epsilon_2 - \epsilon^{\text{eff}})}, \tag{4.8}$$

$$c_2^{\text{U}} = \frac{\epsilon_1 f_2(\epsilon^{\text{eff}} - \langle\epsilon\rangle)}{(\epsilon_2 - \epsilon_1)(\epsilon^{\text{eff}} - \epsilon_1)}. \tag{4.9}$$

Let $\epsilon_1 = 1$ and $\epsilon_2 = 1+\delta$. Using the expansion (2.2), the asymptotic behavior when $\delta \to 0$ is

$$c_2^{\mathrm{U}} - c_2^{\mathrm{L}} = -\frac{c_2(c_2 + f_1 f_2)}{f_1 f_2}\delta + O(\delta^2). \tag{4.10}$$

For a fixed δ, the difference is smaller when the c_2 parameter is close to the end points (3.1). The difference is large when the volume fraction $c_1 = f_1$ is close to the end points, but then the one-point bounds (2.9) and (2.10) are close together.

Remember that the structural parameter c_2 depends on the correlation function $S_2(\boldsymbol{x}_1, \boldsymbol{x}_2)$. The two-point function S_2 can be obtained by randomly tossing line segments of length $|\boldsymbol{x}_1 - \boldsymbol{x}_2|$ with a specified orientation and counting the fraction of times both end points fall in phase 1. The two-point function S_2 can be computed using various methods, see [29, Chapter 12].

4.3 Three-point bounds

Denote by c_3 one of the diagonal elements in $\mathbf{c}_3$. Using the relations (2.15), the three-point lower bound (2.13) is explicitly written

$$\epsilon_3^{\mathrm{L}} = \epsilon_1 \frac{P_3}{Q_3}, \tag{4.11}$$

where the numerator and the denominator are

$$\begin{aligned} P_3 &= \epsilon_2[c_3(\epsilon_1 - \epsilon_2) + c_2(\epsilon_1 - 2\langle\epsilon\rangle) + f_1 f_2 \langle\epsilon\rangle], \\ Q_3 &= c_2^2(\epsilon_1 - \epsilon_2)^2 - f_1 f_2 \epsilon_1 \epsilon_2 + c_2\epsilon_1(\epsilon_1 - \epsilon_2 - \langle\epsilon\rangle) + c_3(\epsilon_1 - \epsilon_2)(f_2\epsilon_1 + f_1\epsilon_2). \end{aligned}$$

The three-point upper bound (2.14), on the diagonal element ϵ^{eff}, is given by

$$\epsilon_3^U = \frac{c_2(\epsilon_1 - \epsilon_2)^2 - c_3(\epsilon_1 - \epsilon_2)\langle\epsilon\rangle + c_2\epsilon_2\langle\epsilon\rangle}{c_2\epsilon_2 + c_3(\epsilon_2 - \epsilon_1)}. \tag{4.12}$$

The structural parameter c_3 can be calculated using differentiation but we need a large number of computations and even then the accuracy in many cases is poor. As above we suggest another approach. Regard $\epsilon_3^{\mathrm{U}}(c_3; \epsilon_1, \epsilon_2, f_1, c_2)$ as a function of c_3 alone. Assume that $c_2 \neq 0$. As above we can prove that the continuous and decreasing function

$$\epsilon_3^{\mathrm{U}} : [\frac{c_2^2}{f_1}, -c_2\left(1 + \frac{c_2}{f_2}\right)] \to [\epsilon_2^{\mathrm{L}}, \epsilon_2^{\mathrm{U}}] \tag{4.13}$$

is a bijection. The inverse $(\epsilon_3^{\mathrm{U}})^{-1}$ is a decreasing function of c_3. This gives $c_3^{\mathrm{U}} := (\epsilon_3^{\mathrm{U}})^{-1}(\epsilon^{\mathrm{eff}}) \geq c_3$ where

$$c_3^{\mathrm{U}} = c_2 \frac{c_2(\epsilon_1 - \epsilon_2)^2 + \epsilon_2(\langle\epsilon\rangle - \epsilon^{\mathrm{eff}})}{(\epsilon_1 - \epsilon_2)(\langle\epsilon\rangle - \epsilon^{\mathrm{eff}})}. \tag{4.14}$$

Using ϵ_3^{L} we obtain in the same way the lower bound

$$c_3^{\mathrm{L}} = \frac{G_3}{H_3}, \tag{4.15}$$

where the two polynomials G_3 and H_3 are

$$\begin{aligned} G_3 &= c_2^2\epsilon^{\text{eff}}(\epsilon_1-\epsilon_2)^2 - \epsilon_1\epsilon_2 f_1 f_2(\epsilon^{\text{eff}} - \langle\epsilon\rangle) + c_2\epsilon_1(\epsilon_2(2\langle\epsilon\rangle - \epsilon_1) + \epsilon^{\text{eff}}(\epsilon_1 - \epsilon_2 - \langle\epsilon\rangle)) \\ H_3 &= (\epsilon_1-\epsilon_2)(\epsilon_1\epsilon_2 - \epsilon^{\text{eff}}(\epsilon_1 f_2 + \epsilon_2 f_1)). \end{aligned}$$

Let $\epsilon_1 = 1$ and $\epsilon_2 = 1+\delta$. Using the expansion (2.2), the asymptotic behavior when $\delta \to 0$ is

$$c_3^{\text{U}} - c_3^{\text{L}} = \frac{(c_3 f_1 - c_2^2)(c_3 f_2 + c_2 f_2 + c_2^2)}{c_2(c_2 + f_1 f_2)}\delta + O(\delta^2). \tag{4.16}$$

For a fixed δ, the difference appers to be smaller when the c_3 parameter is close to the end points (3.2). The difference is large when the c_2 parameter is close to its end points, but then the two-point bounds (2.11) and (2.12) are close together.

Alternatively we could have used that the Padé approximants are Moebius transformations (linear fractional transformations) to show properties (invertability, monotonicity) of the function $\epsilon_{p,q}(c_n)$.

The structural parameter c_3 depends on the two-point function S_2 and the three-point function S_3. The three-point function $S_3(\boldsymbol{x}_1, \boldsymbol{x}_2, \boldsymbol{x}_3)$ is the probability of a triangle having all three vertices in the component 1 material, when placed randomly in the composite at fixed orientation, *i.e.*, over all translations of the triangle. Methods to compute the three-point function S_3 are presented in [29, Chapter 12].

In the case of an isotropic medium we have $\mathbf{c}_3 = f_1 f_2 d^{-2}(f_2 + (d-1)\zeta_1)\mathbf{I}$. This gives us bounds on the parameter ζ_1, using analogous methods.

5 Complex bounds on the permittivity

The $\epsilon_{p,q}$ Padé approximant is of the form

$$\epsilon_{p,q}(c_n) = \alpha_0 + \frac{\alpha_1 c_n + \alpha_2}{\alpha_3 c_n + \alpha_4}. \tag{5.1}$$

Regard α_0, α_1, α_2, α_3 and α_4 as complex numbers. Then (5.1) is the sum of a translation and a Moebius transformation. The real segment $l = \{c_n; c_n^{\min} \le c_n \le c_n^{\max}\}$ is easily seen to be mapped on a circle or a line segment, see [10, p. 200]. For example we get complex bounds from the lens-shaped region bounded by

$$\epsilon_3^{\text{L}}(\tilde{c}_3; \epsilon_1, \epsilon_2, \tilde{c}_2), \quad \epsilon_3^{\text{U}}(c_3; \epsilon_1, \epsilon_2, c_2) \tag{5.2}$$

where the structural parameter $\tilde{c}_3$ varying between

$$-\tilde{c}_2\left(1 + \frac{\tilde{c}_2}{f_1}\right) \le \tilde{c}_3 \le \frac{\tilde{c}_2^2}{f_2} \tag{5.3}$$

and c_3 varying between

$$\frac{c_2^2}{f_1} \le c_3 \le -c_2\left(1 + \frac{c_2}{f_2}\right). \tag{5.4}$$

Alternatively, we can describe the bounds in terms of the points through which the circle passes. Let $\mathrm{Arc}(z_1, z_2, z_3)$ denote the arc of a circle joining the end points z_1 and z_2 that when extended passes through z_3. Such an arc is described by

$$z(t) = z_1 + \frac{1-t}{1/(z_2-z_1) + t/(z_1-z_3)}, \quad 0 \le t \le 1. \tag{5.5}$$

The effective permittivity ϵ^{eff} is bounded by $\mathrm{Arc}(\epsilon_3^{\mathrm{L}}, \epsilon_3^{\mathrm{U}}, \epsilon_2^{\mathrm{L}})$ and $\mathrm{Arc}(\epsilon_3^{\mathrm{L}}, \epsilon_3^{\mathrm{U}}, \epsilon_2^{\mathrm{U}})$. Tighter bounds are given by $\mathrm{Arc}(\epsilon_4^{\mathrm{L}}, \epsilon_4^{\mathrm{U}}, \epsilon_3^{\mathrm{L}})$ and $\mathrm{Arc}(\epsilon_4^{\mathrm{L}}, \epsilon_4^{\mathrm{U}}, \epsilon_3^{\mathrm{U}})$. This was shown in [8, 18] but is here given in terms of Padé approximations that relate the bounds to the structural parameters c_n.

6 Cross-property bounds

The bounds on the effective permittivity can be considerably improved if we have information from experiments. The measurements can be on the material at a different temperature or for a related parameter, such as the magnetic permeability or the thermal conductivity. The important thing is that the microstructure is the same. Assume that we know the value of the parameter at the two phases $\hat{\epsilon}_1$, $\hat{\epsilon}_2$ and the effective parameter $\hat{\epsilon}^{\mathrm{eff}}(\hat{\epsilon}_1, \hat{\epsilon}_2)$. The task is here to infer bounds on $\epsilon^{\mathrm{eff}}(\epsilon_1, \epsilon_2)$. The bounds incorporate knowledge from measurements of a related parameter and they are called cross-property bounds.

Require that the cross-property bounds satisfy

$$\epsilon_1^{\mathrm{U}}(\epsilon_1, \epsilon_2, \hat{c}_1^{\mathrm{U}}) = \epsilon_1^{\mathrm{L}}(\epsilon_1, \epsilon_2, \hat{c}_1^{\mathrm{L}}) = \hat{\epsilon}^{\mathrm{eff}}, \tag{6.1}$$

when $\epsilon_1 = \hat{\epsilon}_1$ and $\epsilon_2 = \hat{\epsilon}_2$. From the definition in Section 4.1 we have $\epsilon_1^{\mathrm{U}} = \hat{\epsilon}^{\mathrm{eff}}$ when $\hat{c}_1^{\mathrm{U}} = c_1^{\mathrm{U}}(\hat{\epsilon}_1, \hat{\epsilon}_2)$ and $\epsilon_1^{\mathrm{L}} = \hat{\epsilon}^{\mathrm{eff}}$ when $\hat{c}_1^{\mathrm{L}} = c_1^{\mathrm{L}}(\hat{\epsilon}_1, \hat{\epsilon}_2)$. The one-point cross-property bounds are then

$$(\epsilon_1^{\mathrm{L}})_{\mathrm{c}} \le (\epsilon^{\mathrm{eff}})_{\mathrm{c}} \le (\epsilon_1^{\mathrm{U}})_{\mathrm{c}} \tag{6.2}$$

where

$$(\epsilon_1^{\mathrm{L}})_{\mathrm{c}} = \epsilon_1^{\mathrm{L}}(\epsilon_1, \epsilon_2, \hat{c}_1^{\mathrm{L}}), \quad (\epsilon_1^{\mathrm{U}})_{\mathrm{c}} = \epsilon_1^{\mathrm{U}}(\epsilon_1, \epsilon_2, \hat{c}_1^{\mathrm{U}}). \tag{6.3}$$

The numerical bounds $\hat{c}_1^{\mathrm{L}}$ and $\hat{c}_1^{\mathrm{U}}$ from (4.2) are here functions of $\hat{\epsilon}_1$, $\hat{\epsilon}_2$. Explicitly, that is

$$(\epsilon_1^{\mathrm{L}})_{\mathrm{c}} = (\hat{c}_1^{\mathrm{L}}/\epsilon_1 + (1-\hat{c}_1^{\mathrm{L}})/\epsilon_2)^{-1}, \quad (\epsilon_1^{\mathrm{U}})_{\mathrm{c}} = \hat{c}_1^{\mathrm{U}}\epsilon_1 + (1-\hat{c}_1^{\mathrm{U}})\epsilon_2 \tag{6.4}$$

where

$$\hat{c}_1^{\mathrm{L}} = \frac{1/\hat{\epsilon}^{\mathrm{eff}} - 1/\hat{\epsilon}_2}{1/\hat{\epsilon}_1 - 1/\hat{\epsilon}_2}, \quad \hat{c}_1^{\mathrm{U}} = \frac{\hat{\epsilon}_2 - \hat{\epsilon}^{\mathrm{eff}}}{\hat{\epsilon}_2 - \hat{\epsilon}_1}. \tag{6.5}$$

This was first obtained in [5] where the author used a variational principle, see also [21, p. 580]. The method presented above instead relates the measured values to the bounds on the structural parameter c_1.

Similarly, in the two-point case the cross-property bounds are required to satisfy

$$\epsilon_2^{\mathrm{U}}(\epsilon_1, \epsilon_2, c_1, \hat{c}_2^{\mathrm{L}}) = \epsilon_2^{\mathrm{L}}(\epsilon_1, \epsilon_2, c_1, \hat{c}_2^{\mathrm{U}}) = \hat{\epsilon}^{\mathrm{eff}}, \tag{6.6}$$

when $\epsilon_1 = \hat{\epsilon}_1$ and $\epsilon_2 = \hat{\epsilon}_2$. From the definition in Section 4.2 we have $\epsilon_2^{\mathrm{U}} = \hat{\epsilon}^{\mathrm{eff}}$ when $\hat{c}_2^{\mathrm{L}} = c_2^{\mathrm{L}}(\hat{\epsilon}_1, \hat{\epsilon}_2)$ and $\epsilon_2^{\mathrm{L}} = \hat{\epsilon}^{\mathrm{eff}}$ when $\hat{c}_2^{\mathrm{U}} = c_2^{\mathrm{U}}(\hat{\epsilon}_1, \hat{\epsilon}_2)$. The two-point cross-property bounds then are

$$(\epsilon_2^{\mathrm{L}})_{\mathrm{c}} \leq (\epsilon^{\mathrm{eff}})_{\mathrm{c}} \leq (\epsilon_2^{\mathrm{U}})_{\mathrm{c}} \tag{6.7}$$

where

$$(\epsilon_2^{\mathrm{L}})_{\mathrm{c}} = \epsilon_1 \frac{\hat{c}_2^{\mathrm{U}}(\epsilon_1 - \epsilon_2) + f_2\langle\epsilon\rangle}{f_2\epsilon_1 + \hat{c}_2^{\mathrm{U}}(\epsilon_1 - \epsilon_2)}, \quad (\epsilon_2^{\mathrm{U}})_{\mathrm{c}} = \epsilon_2 \frac{\hat{c}_2^{\mathrm{L}}(\epsilon_2 - \epsilon_1) + f_1\langle\epsilon\rangle}{f_1\epsilon_2 + \hat{c}_2^{\mathrm{L}}(\epsilon_2 - \epsilon_1)}. \tag{6.8}$$

The parameters $\hat{c}_2^{\mathrm{L}}$ and $\hat{c}_2^{\mathrm{U}}$ from (4.8) and (4.9) are here functions of $\hat{\epsilon}_1$ and $\hat{\epsilon}_2$. This was first obtained in [23], see also [21, p. 580]. Here we use a new method that relates the measured values to the bounds on the structural parameter c_2. The analytical bounds (3.1) can be useful to check the measured values.

The three-point cross-property bounds are also required to satisfy

$$\epsilon_3^{\mathrm{U}}(\epsilon_1, \epsilon_2, c_1, c_2, \hat{c}_3^{\mathrm{U}}) = \epsilon_3^{\mathrm{L}}(\epsilon_1, \epsilon_2, c_1, c_2, \hat{c}_3^{\mathrm{L}}) = \hat{\epsilon}^{\mathrm{eff}}, \tag{6.9}$$

when $\epsilon_1 = \hat{\epsilon}_1$ and $\epsilon_2 = \hat{\epsilon}_2$. We get the tighter bounds

$$(\epsilon_3^{\mathrm{L}})_{\mathrm{c}} \leq (\epsilon^{\mathrm{eff}})_{\mathrm{c}} \leq (\epsilon_3^{\mathrm{U}})_{\mathrm{c}} \tag{6.10}$$

where

$$(\epsilon_3^{\mathrm{L}})_{\mathrm{c}} = \epsilon_3^{\mathrm{L}}(\epsilon_1, \epsilon_2, c_1, c_2, \hat{c}_3^{\mathrm{L}}), \quad (\epsilon_3^{\mathrm{U}})_{\mathrm{c}} = \epsilon_3^{\mathrm{U}}(\epsilon_1, \epsilon_2, c_1, c_2, \hat{c}_3^{\mathrm{U}}). \tag{6.11}$$

The parameters $\hat{c}_3^{\mathrm{U}}$ and $\hat{c}_3^{\mathrm{L}}$ are here functions of $\hat{\epsilon}_1$, $\hat{\epsilon}_2$. In the three-dimensional isotropic case, $c_2 = -f_1 f_2/3$. This was shown in [5, 6, 21]. The analytical bounds (3.1) and (3.2) can be useful to check the measured values. We can also combine the calculations made in, for example, [28] with a measurement of some effective parameter on the same material to get bounds from (6.10).

Similar to Section 5, the effective permittivity ϵ^{eff} is in the complex case bounded by the lens-shaped region

$$\mathrm{Arc}((\epsilon_2^{\mathrm{L}})_{\mathrm{c}}, (\epsilon_2^{\mathrm{U}})_{\mathrm{c}}, (\epsilon_1^{\mathrm{L}})_{\mathrm{c}}), \quad \mathrm{Arc}((\epsilon_2^{\mathrm{L}})_{\mathrm{c}}, (\epsilon_2^{\mathrm{U}})_{\mathrm{c}}, (\epsilon_1^{\mathrm{U}})_{\mathrm{c}}). \tag{6.12}$$

Tighter bounds are given by

$$\mathrm{Arc}((\epsilon_3^{\mathrm{L}})_{\mathrm{c}}, (\epsilon_3^{\mathrm{U}})_{\mathrm{c}}, (\epsilon_2^{\mathrm{L}})_{\mathrm{c}}), \quad \mathrm{Arc}((\epsilon_3^{\mathrm{L}})_{\mathrm{c}}, (\epsilon_3^{\mathrm{U}})_{\mathrm{c}}, (\epsilon_2^{\mathrm{U}})_{\mathrm{c}}). \tag{6.13}$$

6.1 Numerical example

We give an example in the anisotropic and periodic case. Figure 2 shows the complex cross-property bounds for ϵ^{eff} when $f_1 = 0.6$, $\epsilon_1 = 3 + 0.1\mathrm{i}$, $\epsilon_2 = 2 + 20\mathrm{i}$, $\hat{\epsilon}_1 = 1.44$, $\hat{\epsilon}_2 = 160$, and $\hat{\epsilon}^{\mathrm{eff}} = 2.72$ are known constants and the inclusion is placed in a square lattice. The numerical values on ϵ_1 and $\hat{\epsilon}_1$ simulate the permittivity and the thermal conductivity of epoxy, respectively. Simularly, the numerical values on the inclusion corresponds to the permittivity ϵ_2 and thermal conductivity $\hat{\epsilon}_2$ of a carbon material.

The dashed line is the lens-shaped region given by (6.12), which depends on the one-point bounds (6.5) and the two-point bounds (6.7). Tighter bounds are given

	$\hat{c}_1^{\mathrm{L}}$	$\hat{c}_1^{\mathrm{U}}$	c_1	$\hat{c}_2^{\mathrm{L}}$	$\hat{c}_2^{\mathrm{U}}$	c_2	$\hat{c}_3^{\mathrm{L}}$	$\hat{c}_3^{\mathrm{U}}$
$(\epsilon_1^{\mathrm{L}})_{\mathrm{c}}$	0.5251	-	-	-	-	-	-	-
$(\epsilon_1^{\mathrm{U}})_{\mathrm{c}}$	-	0.9919	-	-	-	-	-	-
$(\epsilon_2^{\mathrm{L}})_{\mathrm{c}}$	-	-	0.6	-	-0.1764	-	-	-
$(\epsilon_2^{\mathrm{U}})_{\mathrm{c}}$	-	-	0.6	-0.2392	-	-	-	-
$(\epsilon_3^{\mathrm{L}})_{\mathrm{c}}$	-	-	0.6	-	-	-0.1841	0.09234	-
$(\epsilon_3^{\mathrm{U}})_{\mathrm{c}}$	-	-	0.6	-	-	-0.1841	-	0.09931

Table 1: Illustration of which structural parameters that are used to calculate the different cross-property bounds.

by the solid line, (6.13), which depends on the two-point bounds (6.7) and the three-point bounds (6.10). The n-point bounds depend on the structural parameters, up to and including c_{n-1}, and bounds on the structural parameters $\hat{c}_n$. This dependency and the numerical values are presented in Table 1.

The tighter bounds (6.13) depend on the structural parameter c_2, that here is calculated as the mean value of (4.8) and (4.9), when $\epsilon_1 = 1$, $\epsilon_2 = 1.01$ and $\epsilon^{\mathrm{eff}} = 1.0039817$. The numerical calculation of c_2 require many digits of ϵ^{eff} for this small contrast. In practice, image analysis can also be used to calculate c_2, see [29, Chapter 12]. The effective parameter $\hat{\epsilon}^{\mathrm{eff}}$ is calculated numerically, but can also be the result of a measurement of, for example, the thermal conductivity.

The end point $(\epsilon_3^{\mathrm{L}})_{\mathrm{c}} = 5.4091+1.0381\mathrm{i}$ is close to the correct effective permittivity $\epsilon^{\mathrm{eff}} = 5.3837 + 1.0465\mathrm{i}$. This comes as no surprise because inclusions cannot heavily influence the effective parameter when we are below percolation threshold, see [17].

The numerical calculations of the effective parameters from the local problem, [2, p. 663], were done with FEMLAB (`www.comsol.com`).

7 Discussion and conclusions

The numerical bounds on the structural parameters in Section 4 are sometimes broad and sometimes very narrow, depending on the contrast and the geometry. Calculations of the structural parameters give us physical understanding on the problem and can be used to check calculations based on image analyses.

The new analytical bounds in Section 3 give us the possibility to see which effective parameters of the composite materials that are possible to achieve, given some of the structural parameters $\mathbf{c}_n$.

The new cross-property bounds in Section 6 give us narrow bounds from one measurement of some effective parameter together with a measurement of the two-point correlation function S_2, see (2.3).

Many of the results given here can easily be extended. Numerical calculations and comparison with results from measurements are currently being undertaken.

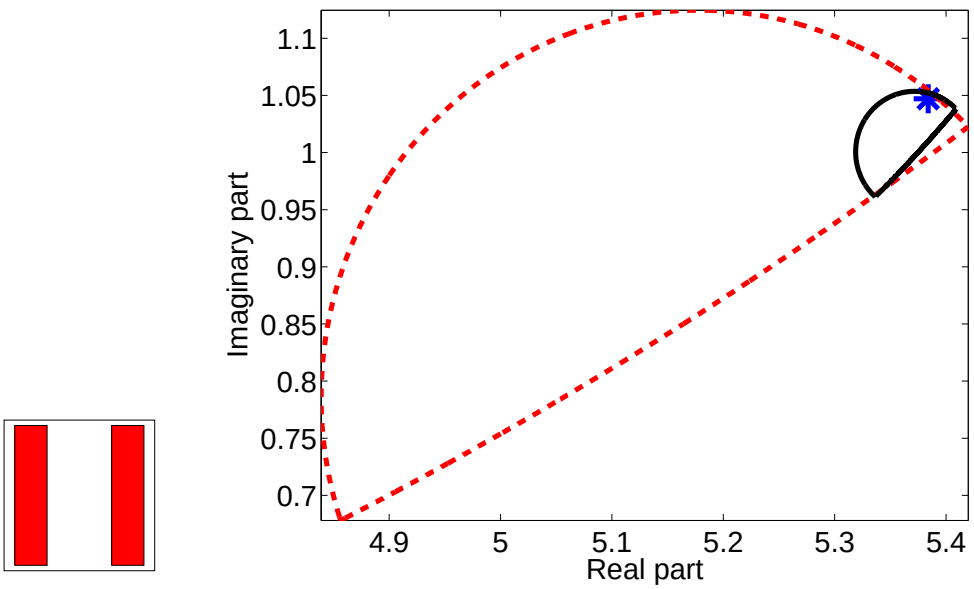

Figure 2: The applied field is oriented perpendicularly to the rods. The effective permittivity ϵ^{eff} is bounded by the dashed line (6.12) and tighter bounds are given by the solid line (6.13). The star is the effective permittivity calculated from the local problem.

References

[1] G. A. Baker. *Essentials of Padé Approximants*. Academic Press, New York, 1975.

[2] A. Bensoussan, J. L. Lions, and G. Papanicolaou. *Asymptotic Analysis for Periodic Structures*, volume 5 of *Studies in Mathematics and its Applications*. North-Holland, Amsterdam, 1978.

[3] M. J. Beran. Use of the variational approach to determine bounds for the effective permittivity in random media. *Nuovo Cimento*, **38**, 771–782, 1965.

[4] M. J. Beran. *Statistical Continuum Theories*. Interscience Publishers, New York, 1968.

[5] D. J. Bergman. Variational bounds on some bulk properties of a two-phase composite material. *Phys. Rev. B*, **14**(4), 1531–1542, 1976.

[6] D. J. Bergman. The dielectric constant of a composite material - a problem in classical physics. *Physical Reports*, **43**(9), 377–407, 1978.

[7] D. J. Bergman and K.-J. Dunn. Bulk effective dielectric constant of a composite with a periodic microgeometry. *Phys. Rev. B*, **45**(23), 262–271, 1992.

[8] D. J. Bergman. Bounds for the complex dielectric constant of a two-component composite material. *Phys. Rev. B*, **23**(6), 3058–3065, 1981.

[9] W. F. Brown. Solid mixture permittivities. *J. Chem. Phys.*, **23**(8), 1514–1517, 1955.

[10] S. D. Fisher. *Complex variables*. Wadsworth & Brooks, Pacific Grove, CA, 1990.

[11] Z. Hashin and S. Shtrikman. A variational approach to the theory of the effective magnetic permeability of multiphase materials. *J. Appl Phys.*, **33**(10), 3125–3131, 1962.

[12] J. Helsing. Fast and accurate calculations of structural parameters for suspensions. *Proc. Roy. Soc. London Ser. A*, **445**, 127–140, 1994.

[13] J. Helsing. Thin bridges in isotropic electrostatics. *Journal of Computational Physics*, **127**(1), 142–151, 1996.

[14] J. Helsing. A high-order accurate algorith for electrostatics of overlapping disks. *J. Stat. Phys.*, **90**(5–6), 1461–1473, 1998.

[15] R. V. Kohn and G. W. Milton. On bounding the effective conductivity of anisotropic composites. In J. L. Ericksen, D. Kinderlehrer, R. Kohn, and J.-L. Lions, editors, *Homogenization and Effective Moduli of Materials and Media*, volume 1 of *IMA Volumes in Mathematics and Its Applications*, pages 97–125. Springer-Verlag, Berlin, 1986.

[16] K. A. Lurie and A. V. Cherkaev. Exact estimates of conductivity of composites. *Proc. Royal Soc. Edinburgh*, **A99**, 71–84, 1984.

[17] R. C. McPhedran and G. W. Milton. Bounds and exact theories for the transport properties of inhomogeneous media. *Applied Physics A*, **26**(4), 207–220, 1981.

[18] G. W. Milton. Bounds on the transport and optical properties of two-component composite material. *J. Appl Phys.*, **52**(8), 5294–5304, 1981.

[19] G. W. Milton. Multicomponent composites, electrical networks and new types of continued fraction. I. *Communications in Mathematical Physics*, **111**(2), 281–327, 1987.

[20] G. W. Milton. Multicomponent composites, electrical networks and new types of continued fraction. II. *Communications in Mathematical Physics*, **111**(3), 329–372, 1987.

[21] G. W. Milton. *The Theory of Composites*. Cambridge University Press, Cambridge, U.K., 2002.

[22] D. C. Pham and S. Torquato. Strong-contrast expansions and approximations for the effective conductivity of isotropic multiphase composites. *J. Appl Phys.*, **94**(10), 6591–6601, 2003.

[23] S. Prager. Improved variational bounds on some bulk properties of a two-phase random medium. *J. Chem. Phys.*, **50**(10), 4305–4312, 1969.

[24] J. Quintanilla and S. Torquato. Microstructure and conductivity of hierarchical laminate composites. *Phys. Rev. E*, **53**, 4368–4378, 1992.

[25] A. K. Sen and S. Torquato. Effective conductivity of anisotropic two-phase composite media. *Phys. Rev. B*, **39**(7), 4504–4515, 1989.

[26] N. R. Silnutzer. *Effective constants of statistically homogeneous materials.* PhD thesis, University of Pennsylvania, Philadephia, 1972.

[27] L. Tartar. Estimations fines de coefficients homoqénéisés. In P. Krée, editor, *Ennio De Giorgi Colloquium, Research Notes in Mathematics 125*, pages 168–187, 1985.

[28] S. Torquato and A. K. Sen. Conductivity tensor of anisotropic composite media from the microstructure. *J. Appl Phys.*, **67**(3), 1145–1155, 1990.

[29] S. Torquato. *Random Heterogeneous Materials: Microstructure and Microscopic Properties.* Springer-Verlag, Berlin, 2002.

[30] O. Wiener. Die Theorie des Mischkörpers für das Feld des stationären Strömung. *Abh. Math. -Physichen Klasse Königl. Sächsh. Gesel. Wissen*, **32**, 509–604, 1912.